Null Test of Newtonian Inverse-Square Law at Submillimeter Range with a Dual-Modulation Torsion Pendulum

Liang-Cheng Tu, Sheng-Guo Guan, Jun Luo,* Cheng-Gang Shao, and Lin-Xia Liu

Department of Physics, Huazhong University of Science and Technology, Wuhan 430074, People's Republic of China

(Received 7 January 2007; revised manuscript received 28 March 2007; published 14 May 2007)

A null experimental test of the Newtonian inverse-square law at submillimeter range using a torsion pendulum was presented. Under the dual modulations of both the expected signal and the gravitational torque for calibration, our data concluded with 95% confidence that no new forces were observed and any gravitational-strength Yukawa forces ($|\alpha| \geq 1$) must have a length scale $\lambda < 66\ \mu$m, agreeing well with the latest result of the Eöt-wash group. Our result sets a unification energy scale of $M^* \geq 2.8\ \mathrm{TeV}/c^2$ for the two compactified extra space dimensions with the same size $R^* < 47\ \mu$m.

DOI: 10.1103/PhysRevLett.98.201101 PACS numbers: 04.80.Cc

Newtonian gravitational interaction at length scales down to several submillimeters has aroused considerable interest recently under mainly two hierarchy problems of gravity: the gauge hierarchy problem of 10^{16} times discrepancy between the standard model (SM) energy scale $M_{\mathrm{SM}} \approx 1\ \mathrm{TeV}/c^2$ and the Planck scale $M_P \approx \sqrt{\hbar c/G} = 1.2 \times 10^{16}\ \mathrm{TeV}/c^2$ [1,2]; the cosmological constant problem of at least 10^{60} times smallness between the observed gravitating energy density and the predicted vacuum energy density [3–5]. Various theories of physics beyond the SM hence predicted new behaviors of gravitation at short length scales below 1 mm, and suggested that the existence of the extra time-space dimensions or new interactions from the exchange of proposed exotic particles weakens the strength of gravity. Of particular interest to us is the theoretical predictions of Arkani-Hamed, Dimopoulos, and Dvali (ADD) theory [1] that the size of the compactified extra space dimensions could be large enough to an experimental measurable range, while the gravitation would deviate the inverse-square law at distances comparable to the radii R^* of the extra dimensions with $R^* = \hbar c/(2\pi M^* c^2)(M_P/M^*)^{2/n}$, where M^* is the unification energy scale and n is the number of the compactified extra dimensions. To lower M^* to M_{SM}, for $n = 1$, $R^* \approx 10^{12}$ m has been ruled out by solar-system observations [6]. For two extra space dimensions, $R^* \approx 0.3$ mm is of interest and accessible for tabletop experiments.

In the presence of non-Newtonian interactions, the gravitational potential is usually modified by adding a Yukawa term into the standard Newtonian one as [1]

$$V(r) = -G\frac{m_1 m_2}{r}(1 + \alpha e^{-r/\lambda}), \tag{1}$$

where G is the gravitational constant, m_1 and m_2 are the two point masses separated by distance r, and α is the dimensionless strength of non-Newtonian potential relative to gravity with a length scale λ. Experimental tests of Yukawa type gravity are usually parameterized by setting stringent constraints on the $|\alpha|$-λ space [7].

This Letter reports the result of our test of non-Newtonian gravitational interactions for surface separations between two parallel thin gold rectangular plates down to 176 μm with a torsion pendulum, and the schematic diagram is shown in Fig. 1.

The pendulum consisted of five rectangular K9 glass blocks. The main one is the body of the pendulum with dimensions $99.97 \times 19.93 \times 11.98\ \mathrm{mm}^3$. Two glass bases of $20.06 \times 20.08 \times 1.986\ \mathrm{mm}^3$ attached on both ends of the body at one surface were used to protrude the gold test mass of $19.98 \times 20.07 \times 0.202\ \mathrm{mm}^3$ and correspondingly counterbalance one of $20.09 \times 20.06 \times 0.205\ \mathrm{mm}^3$, respectively. Because of this design, the electrostatic effect between the body and the glass membrane frame (GMF) can be greatly reduced. The last two glass blocks of $19.47 \times 19.46 \times 3.58\ \mathrm{mm}^3$ attached on the other surface of the body were both acted as counterbalance for keeping the symmetry of the pendulum. All the above parts were connected with the optical adhesive solidified by the ultraviolet light, and then the pendulum was coated with gold to minimize the variations of the electrostatic potential on its surface. The pendulum of total mass 79.633 g was suspended from an annealed tungsten fiber of 568 mm in length and 25μm in diameter by means of a small cylindrical aluminum clamp, which was aligned to the center of the pendulum by an Abbe comparator with an uncertainty of 10 μm. The upper end of the torsion fiber was attached to the copper disk of the magnetic damper system, which was used to suppress the simple pendulum motions [8]. The copper disk was suspended by a 51-mm-long, 50-μm-diameter annealed tungsten prehanger fiber, which was finally fixed to a vacuum feedthrough fastened on a XYZ compact stage on the top of the vacuum vessel.

The gold-coated source mass platform consisted of three parts. The first part is a pure gold block of $18.00 \times 17.24 \times 0.210\ \mathrm{mm}^3$ that acted as source mass, which was stuck on an equal-area glass block with the thickness of 2.007 mm. The second is a gravitational compensating glass block of $17.70 \times 17.02 \times 19.99\ \mathrm{mm}^3$, which was used to compensate the change of Newtonian gravitational torque, pro-

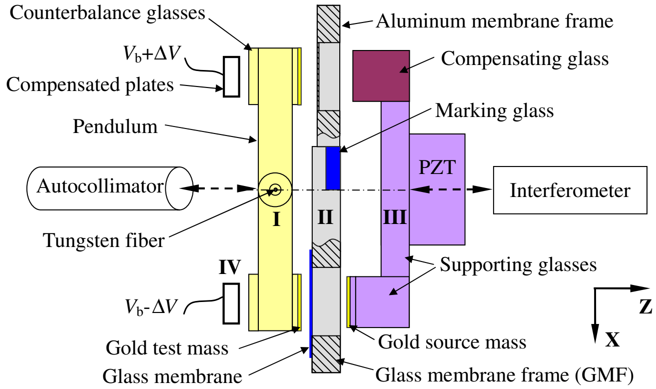

FIG. 1 (color online). Schematic top view of the experimental setup which was constituted by four separate parts, the pendulum (I), the membrane frames (II), the source mass platform (III), and the electrostatic compensated plates (IV). The II and III parts were mounted on a 6 degree-of-freedom stage (not shown here) together while the III part was then fixed on an X-Z translation stages (not shown) and finally on a PZT. The pendulum twist and the movement of the source mass were monitored by a two-axis autocollimator and the Michelson interferometer, respectively. Source mass motion was in the Z direction.

duced by all movable parts of the source mass platform during moving forwards or backwards in the testing range, to less than 2.1×10^{-16} N m, and a prefect cancellation was designed at the gap of 250 μm between the test mass and source mass. However, the expected non-Newtonian gravitational effect could not be reduced by the compensating block due to larger separation compared with that of the source mass. This design leads to a null test of the expected signal. The third part is the symmetrical supporting glasses which were used to support the former two parts and connected with the piezoelectric translator (PZT), and the net gravitational torque change acting on the pendulum produced by it due to moving forward and backward is less than 3.7×10^{-17} N m.

Between the test mass and the source mass, there were two gold-coated membrane frames (as shown in Fig. 1). The GMF ($80.00 \times 60.00 \times 10.00$ mm^3) with a 31-mm-diameter hole, covered by a gold-coated glass membrane of 56 μm in thickness and 38 mm in diameter, was used to nest the source mass and minimize the electrostatic torque acted on the pendulum. For the same reason, an aluminum membrane frame of $50.00 \times 60.00 \times 8.00$ mm^3 located behind the glass one about 2 mm, had a hollowed out cavity of 31-mm diameter also to nest the gravitational counterbalance mass.

All the glass blocks used were elaborately ground and polished under the same controlled standard of flatness ≤ 0.06 μm, parallelism ≤ 2 arcsec, and verticality ≤ 20 arcsec. The parameters including the dimensions and masses of the blocks were determined precisely by a length comparator of 80 nm accuracy and an electronic balance of 0.1 mg resolution. During preparation of the pendulum and the source mass platform, four standard glass gauges (two parallel rulers and two triangular ones, a plane with flatness of <0.06 μm and angle with verticality of <0.2 arcsec) were used to keep the alignment of each glass/gold block. The relative positions of all parts composing the pendulum and the source mass platform were measured individually by an optical-vision-measuring system with a resolution of 2 μm, while the parallelisms were controlled under the two-axis autocollimator with a resolution of 0.01 arcsec.

The GMF was also used as the reference to transfer both the parallelism ($\Delta\theta^x_{ps}$, $\Delta\theta^y_{ps}$, $\Delta\theta^z_{ps}$, hereafter the subscripts p, s, m denoted the pendulum, the source mass, the GFM, respectively) and the relative positions (Δx_{ps}, Δy_{ps}, Δz_{ps}) between the pendulum and the source mass platform. The entire source mass platform including the PZT was installed on an X-Z translation stage with a resolution of 1 μm to adjust the horizontal displacements between the gold source mass and the GMF, which were all fixed on the same aluminum base mounted on 6-DOF stage (with the resolutions of 0.36 arcsec for the circle goniometer and 0.05 μm for the linear displacement) in the vacuum vessel. For the parallelism between the source mass and the GMF $\Delta\theta^x_{sm}$, $\Delta\theta^y_{sm}$, the two-axis autocollimator was used while installing the source mass platform on the aluminum base, and finally parallelisms of less than 3 arcsec were achieved. The height difference between the upper surface of the GMF and the source mass $\Delta\theta^z_{sm}$ was determined by a depth micrometer with an accuracy of 50 arcsec. Then, the separation between the left surfaces of the source mass and the GMF was set to $\Delta z_{sm} = (48 \pm 2)$ μm.

The attitude of the free pendulum around the x axis $\Delta\theta^x_p$ was measured by the x axis of the autocollimator. The GMF was then adjusted to $\Delta\theta^x_m \approx \Delta\theta^x_p$ within 1 arcsec by the 6-DOF stage after the pendulum was elevated by the XYZ compact stages, while the parameter $\Delta\theta^y_m$, output from the y axis of the autocollimator, was fixed as the reference plane of the pendulum in succeeding alignments and experiments. The size of $\Delta\theta^z_{pm}$ was determined by lowering the pendulum to touch the top surface of GMF, then the 6-DOF stage was rotated until the other end touched. Several times of lowering and rotating resulted in $\Delta\theta^z_{pm} \leq 34$ arcsec. By attaching a marking glass block on the top of GMF with its side at the middle of the source mass platform in the x direction, the uncertainty Δx_{ps} was minimized to $\sim$25 μm by shifting the 6-DOF stage until the fiber of the pendulum and the marking glass block were exactly overlapped by an optical level gauge located at the orthogonal direction to the GMF. The Δy_{ps} was also limited within 25 μm by another optical level gauge monitoring the height of the pendulum and the GMF.

After the above procedures were finished, the PZT and the 6-DOF stage were enveloped together with a pure aluminum membrane to minimize electrostatic interactions. Finally, two electrostatic compensated plates with conical shape were mounted on the vacuum vessel facing to the counterbalance glass blocks (as shown in the Fig. 1) with a gap of $\sim$12 mm to form the differentially parallel capacitors, respectively. They were used to keep the tungsten fiber always untwisted by applying differential voltages ($V_- = V_b - \Delta V$ and $V_+ = V_b + \Delta V$ where a forward bias V_b was set to 5 V) on the plates. Thus the applied voltage ΔV reflected the torques generated by the interactions including Newtonian gravity and all other possible short-range forces between the source masses and the pendulum.

The entire system was maintained at a vacuum of $\sim 10^{-5}$ Pa located in our cave laboratory [9]. During acquisition of the vacuum, the relative positions of the pendulum to the source masses changed with the deformation of the vessel due to differential atmosphere pressure, and hence three optical level gauges isolated from the vessel table were set up to monitor the changes and the pendulum was adjusted to its original position finally.

The pendulum-membrane separation was first set at $\sim$3 mm by moving backwards the 6-DOF stage. The free motion of the pendulum was recorded while the entire system was earthed, which indicated a free oscillation period of $T_0 = (551.82 \pm 0.01)$ s, yielding the fiber's torsional spring constant $k_f = (9.64 \pm 0.02) \times 10^{-9}$ N m/rad by considering the calculated rotational inertia momentum of the pendulum $I_p = (7.43 \pm 0.02) \times 10^{-5}$ kg m^2. A copper cylinder mounted on a turntable outside of the vessel, whose rotation axis is in the vertical direction and about 450 mm away from the tungsten fiber, was rotated continuously at a period of 1800 s ($f_c = 0.556$ mHz) with a rotation radius of 120 mm. The torque amplitude at f_c was determined by the fitting the data with the expected signal based on least squared method, and yielded $\tau_{co} = (2.49 \pm 0.08) \times 10^{-14}$ N m at f_c, which was constant and hence used to calibrate the compensated voltage when the pendulum was running on the closed-loop performance subsequently.

Then, the source mass together with the frames was comoved forwards to approach the pendulum until the spacing between the test mass and the left surface of the GMF was $\Delta z_{pm} = (69 \pm 3)$ μm, which was determined by monitoring the rotating angles of the pendulum when the edge of the pendulum contacted with the glass membrane. Several attempts to achieve a smaller separation did not succeed due to the abruptly increased electrostatic effect. The differential capacitive transducer was then run to restrict the pendulum twist with the measured $\Delta\theta_m^y$ as the reference position by applying the compensated voltage ΔV. After the pendulum was under control, various voltages were applied to the GMF to find the residual potential on the pendulum ($V_{\rm rp} = 73.8$ mV), Then a compensating voltage was applied to the GMF to maintain zero differential potential between them.

Finally, the PZT was driven continuously by an applied trapezoidal wave voltage, which was used to modulated the separation between the test and source masses, and hence the expected non-Newtonian gravitational torque acting on the closed-loop pendulum. The moving period of the PZT was chosen to be 2160 s ($f_s = 0.463$ mHz), which moved the source mass with a displacement of (165 ± 3) μm, corresponding to the separation changing from 176 to 341 μm between the test mass and the source mass. At the two ends of the movement, the PZT was maintained invariable voltages for 60 s to help it extend and shrink fully. The calibrating copper cylinder was rotating synchronously with the frequency of f_c acting as a diagnostic modulation. The amplitude of ΔV at f_c was (99.1 ± 8.5) mV, and hence yielded the calibrated coefficient of $\beta = (2.51 \pm 0.23) \times 10^{-16}$ N m/mV for the torque vs ΔV acting on the pendulum. Our first attempts at shorter periods were unsuccessful and a false torque with fundamental frequency occurred. This signal, arising from the sudden disturbances of the electrostatic interactions between the source mass and the membrane at the closest spacing, vanished when the movement of the source mass was slowed down. The experimental signals, including the outputs from the autocollimator, the capacitive transducer, the Michelson interferometer, six temperature sensors, and one barometer, were collected continuously by the data acquisition system.

Experimental data were accumulated at a sampling rate of 1 Hz. For 13 recorded valid segments, the duration of each data sample was over 40 h. Converting the voltage applied on the capacitive transducer to the compensated torque, a typical power spectral density was shown in Fig. 2. The uncertainties of δf_c, δf_s, and the resolution of FFT δf were 5.5×10^{-8}, 2.2×10^{-8}, and 6.9×10^{-6} Hz, respectively. For all the segments of valid data, the calibrating amplitude at f_c was well consistent, and hence was used to determine the mean noise density at f_s correspondingly. From Fig. 2, the mean noise density at f_s could be determined as 9.5×10^{-14} N m/$\sqrt{\rm Hz}$. We conservatively selected the δf as the bandwidth to estimate signal magnitude at f_s, and yielded $\Delta\tau_s \leq 2.5 \times 10^{-16}$ N m.

The present sensitivity was basically limited by the ambient electrostatic fluctuation acting on the pendulum, which also restricted the minimal accessible separation. Other nongravitational sources of systematic uncertainty were the variations of the temperature, the magnetic field, and the air pressure. The temperature effect on the pendulum was exaggerated by modulating the environmental temperature, and yielded a thermal coefficient of $(3.7 \pm 0.1) \times 10^{-17}$ N m/mK. The maximal temperature variation at f_s was $\leq$0.2 mK during normal data collecting, indicting that the spurious torque from thermal variation was $< 8 \times 10^{-18}$ N m. The modulation method was used to measure the response of the pendulum to the variation of the magnetic field of two sets of coils using a standard flux-gate magnetometer, and gave $(1.65 \pm 0.02) \times 10^{-16}$ N m/mG. The magnetic field fluctuation at the site

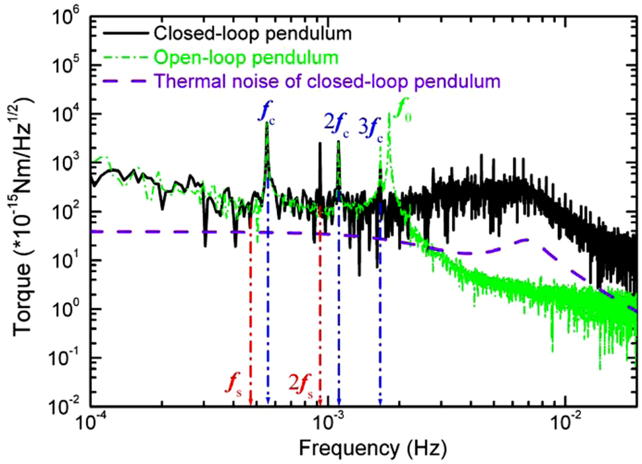

FIG. 2 (color online). Typical power spectral densities of the torque experienced by the open-loop (dash-dot line) and closed-loop (solid line) pendulum. The high-order components of f_c occurred due to the asymmetrically gravitational interaction between the dipole moment pendulum and the rotating cylinder. Under closed-loop, the double signal at $2f_s$ arose from the electrostatic interactions at both the source mass approaching and leaving the pendulum. The sensitivity of our experiment was almost unchanged at the signal frequency of f_s for the open-loop pendulum and the closed-loop one, and the amplitude of closed-loop pendulum exceeded the thermal value (dash) by about a factor of 3, but became worse at higher frequency due to the active electrostatic controller compared with the open-loop one.

of the pendulum was $\leq 8.0\ \mu$G at f_s, corresponding to systematic error torque of $< 2 \times 10^{-18}$ N m. The variations of the air pressure would deformed the vacuum vessel and change the equilibrium position of the pendulum, which yielded a coupling coefficient of $(1.8 \pm 0.1) \times 10^{-17}$ N m/mbar by correlating recorded air pressure with ΔV, and the maximal change of ≤ 0.25 mbar at f_s contributing an error torque $< 5 \times 10^{-18}$ N m.

The measured torque at f_s allowed computation of an experimental constraint on the violations of the Newtonian inverse-square law. The constraint at 95% confidence with $2\Delta\tau_s$ was shown in Fig. 3, which was obtained by the numerical integral of the determinate function between α and λ according to Eq. (1) while knowing the experimental geometrical and mass configuration and the testing range. Our result, closely comparable to that of the Eöt-wash group, concluded that the strength of any gravitylike Yukawa interaction (namely, $|\alpha| = 1$) must have a scale $\lambda < 66\ \mu$m, agreeing well with the latest results of [10]. For one single extra dimension with dimension R predicted by [1,2], the size $\alpha = 8/3$ set an upper limit of $R^* < 53\ \mu$m. Our result also excluded the possibility of two compactified extra space dimensions with the same size at submillimeter scale predicted by ADD theory on the assumption of lowering the fundamental energy scale to $M^* \approx 1$ TeV$/c^2$. For $n = 2$, our result indicated $\alpha < 0.047$ at $R^* = 0.3$ mm, and for $\alpha = 16/3$, our required $R^* < 47\ \mu$m, which implied that the new unification energy scale should be $M^* \leq 2.8$ TeV$/c^2$.

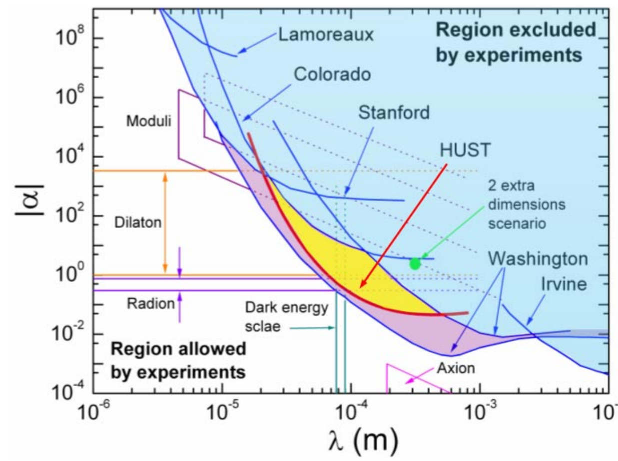

FIG. 3 (color online). Current constraints on the strength of non-Newtonian interaction in $|\alpha|$-λ space between 1 μm to 1 cm range. The previous works have excluded the region with the solid lines labeled by Irvine [11], Washington [10,12], Colorado [13], Stanford [14], and Lamoreaux [15], respectively. The heavy line was our result at the 95% confidence level. Lighter lines showed various theoretical predictions summarized in [7].

This work was supported by the National Basic Research Program of China (No. 2003CB716300) and the National Natural Science Foundation of China (No. 10121503).

*Electronic address: junluo@mail.hust.edu.cn

[1] N. Arkani-Hamed, S. Dimopoulos, and G. Dvali, Phys. Lett. B **429**, 263 (1998); Phys. Rev. D **59**, 086004 (1999).
[2] S. Dimopoulos and G. F. Giudice, Phys. Lett. B **379**, 105 (1996).
[3] S. R. Bennet, Gen. Relativ. Gravit. **29**, 945 (1997).
[4] R. Sundrum, J. High Energy Phys. 07 (1999) 1; Phys. Rev. D **69**, 044014 (2004).
[5] D. B. Kaplan and M. B. Wise, J. High Energy Phys. 08 (2000) 037.
[6] C. Talmadge *et al.*, Phys. Rev. Lett. **61**, 1159 (1988).
[7] E. G. Adelberger, B. R. Heckel, and A. E. Nelson, Annu. Rev. Nucl. Part. Sci. **53**, 77 (2003); J. C. Long *et al.*, Nucl. Phys. **B539**, 23 (1999).
[8] Y. Tu *et al.*, Phys. Lett. A **331**, 354 (2004).
[9] J. Luo *et al.*, Phys. Rev. D **59**, 042001 (1998).
[10] D. J. Kapner *et al.*, Phys. Rev. Lett. **98**, 021101 (2007).
[11] J. K. Hoskins *et al.*, Phys. Rev. D **32**, 3084 (1985).
[12] C. D. Hoyle *et al.*, Phys. Rev. Lett. **86**, 1418 (2001); C. D. Hoyle *et al.*, Phys. Rev. D **70**, 042004 (2004).
[13] J. C. Long *et al.*, Nature (London) **421**, 922 (2003).
[14] J. Chiaverini *et al.*, Phys. Rev. Lett. **90**, 151101 (2003); S. J. Smullin *et al.*, Phys. Rev. D **72**, 122001 (2005).
[15] S. K. Lamoreaux, Phys. Rev. Lett. **78**, 5 (1997).